Diagn Interv Radiol 2025; DOI: 10.4274/dir.2025.253677

EMERGENCY RADIOLOGY

ORIGINAL ARTICLE

©Copyright 2026 Author(s) - Available online at dirjournal.org.
Content of this journal is licensed under a Creative Commons Attribution-NonCommercial 4.0 International License.

The relationship between hypostasis and gas detected in postmortem computed tomography and the postmortem interval

Vefa Çakmak[1]
Abdülkadir İzci[2]
Tuğçe Dönmez[1]
Zeynab Zülfügarlı[1]
Ayşe Kurtuluş Dereli[3]
Kemalettin Acar[3]

[1]Pamukkale University Faculty of Medicine, Department of Radiology, Denizli, Türkiye

[2]Afyonkarahisar Health Sciences University Faculty of Medicine, Department of Forensic Medicine, Afyonkarahisar, Türkiye

[3]Pamukkale University Faculty of Medicine, Department of Forensic Medicine, Denizli, Türkiye

PURPOSE

To evaluate the relationship between gas detected in solid organs, such as the aorta and heart, and hypostasis in the lung parenchyma on postmortem computed tomography (PMCT) in relation to the postmortem interval (PMI).

METHODS

Between January 2021 and January 2025, 74 individuals (60 men, 14 women; 18–84 years; mean age, 41.8 ± 17.6 years) who underwent autopsy due to various forensic causes were retrospectively evaluated using PMCT images obtained prior to autopsy. The presence of gas in the heart, liver, kidneys, and aorta on postmortem thoracic and abdominal CT images was graded as follows: grade 0, absent; grade 1, ≤ 25%; grade 2, > 25% but < 50%; and grade 3, ≥ 50%. These findings were compared with the PMI. In addition, the presence of hypostasis and clotting in the lungs on thoracic PMCT was compared with the PMI.

RESULTS

Intravascular gas was observed within the cardiac chambers in all but seven cases, and the amount of intracardiac gas increased in direct proportion to the PMI. The presence of clotting in the pulmonary arteries showed a statistically significant association with the PMI (P = 0.015). A strong positive correlation (r: 0.720) was identified between intravascular gas in the liver and that in the cardiac chambers. Furthermore, a statistically significant and strong positive correlation was found between pulmonary hypostasis and clotting in the pulmonary arteries (r: 0.892, P = 0.001). A strong correlation was also observed between pulmonary arterial clotting and the density differences between hypostatic and non-hypostatic regions of the lung parenchyma (r: 0.918).

CONCLUSION

On PMCT, decomposition-related gas can be detected in solid organs, particularly in the liver and heart, as early as within 48 hours postmortem, and its presence is associated with the PMI. A strong correlation exists between pulmonary arterial clotting or sedimentation and hypostasis in the lung parenchyma.

CLINICAL SIGNIFICANCE

PMCT can help determine the PMI, in addition to identifying forensic causes of death, and may contribute to routine forensic assessment.

KEYWORDS

Hypostasis, postmortem computed tomography, forensic imaging, autopsy, postmortem interval

Handling editor: Sonay Aydın

Corresponding author: Vefa Çakmak

E-mail: vefacakm1408@gmail.com

Received 30 September 2025; revision requested 21 October 2025; accepted 01 November 2025.

Epub: 24.11.2025

Publication date: 02.11.2026

DOI: 10.4274/dir.2025.253677

You may cite this article as: Çakmak V, İzci A, Dönmez T, Zülfügarlı Z, Kurtuluş Dereli A, Acar K. The relationship between hypostasis and gas detected in postmortem computed tomography and the postmortem interval. *Diagn Interv Radiol.* 2026;32(6):787-793.

Postmortem computed tomography (PMCT) is performed to identify abnormalities that may be overlooked during forensic autopsy and to complement autopsy findings.[1,2] In addition to typical postmortem changes, PMCT can provide ballistic information in firearm injuries, such as bullet localization, type, and trajectory, thereby contributing to the determination of the cause of death. Moreover, PMCT can demonstrate findings related to other forensic cases, such as assault, stab wounds, or penetrating injuries.[3] In countries with a large elderly population, postmortem thoracic CT is particularly useful for detecting lung and cardiovascular pathologies.

Evaluation of the lungs and pleural cavities with PMCT prior to autopsy facilitates the differentiation of certain structural and acquired cardiopulmonary conditions from traumatic pathologies such as contusion or laceration. Pulmonary congestion, which often develops due to cardiac events, appears on CT as ground-glass opacities with peribronchial thickening, whereas pulmonary contusions manifest as ground-glass opacities not conforming to specific segments or distributions. Hypostasis (dependent density), commonly observed in PMCT, may mimic or overlap with these findings. It is characterized by gravity-dependent ground-glass opacities in the lower regions of the lung parenchyma, resulting from higher water content than in other lobes.[4] The presence of hypostasis, a phenomenon that can also be observed in otherwise healthy individuals, varies according to the postmortem interval (PMI).[5]

Main points

- Postmortem computed tomography (PMCT) helps determine the forensic causes of death by providing ballistic information about bullet localization and the type and direction of bullets in firearm injuries, along with radiological findings of assaults, stabbings, and other penetrating injuries.
- In PMCT, the presence of gas in organs caused by putrefaction is moderately correlated with the postmortem interval. Gas is consistently observed in the heart within 0–7 hours after death and in the liver and aorta within 8–16 hours or more.
- In PMCT, hypostasis is demonstrated by the presence of clotting or sediment in the pulmonary arteries, with distribution dependent on the position of the corpse. After approximately 48–72 hours postmortem, pulmonary hypostasis regresses in parallel with the resolution of clotting or sediment in the pulmonary arteries.

During the postmortem period, it has been reported that decomposition-related gas begins to form within 24–48 hours after death, mainly produced by the intestinal flora. Environmental factors, such as body preservation status, ambient temperature, and humidity, also influence gas formation due to putrefaction.[6,7] Even small amounts of intraparenchymal or intravascular gas, which may be difficult to detect at autopsy, can be easily identified on PMCT. It is crucial, however, to distinguish decomposition-related gas from air embolism. Although the distribution of postmortem gas varies depending on the PMI, it is most frequently detected in the liver and heart. In forensic investigations, both the extent of intravascular and parenchymal gas on CT and the presence or absence of pulmonary hypostasis appear to be important indicators for estimating the PMI. Accordingly, we hypothesize that gas formation and pulmonary hypostasis observed on PMCT correlate positively with the PMI.

The aim of this study was to evaluate the relationship between gas and hypostasis detected in organs on PMCT and the PMI.

Methods

Ethical statement

This study was initiated after approval by the Pamukkale University Non-Invasive Clinical Research Ethics Committee (protocol number: E-60116787-020-556684, date: 07/23/2024).

Study group

Between January 2021 and January 2025, PMCT images [number of cases (n) = 84] obtained prior to autopsy from individuals with preserved cranial, thoracic, and abdominal organ integrity in the Radiology Archive of Pamukkale University Faculty of Medicine Hospital were retrospectively reviewed. Cases were excluded if organ integrity was compromised, the body was not found in a supine position, there was evidence of death due to burns or blast injuries, or if the CT images exhibited missing data or extensive artifacts.

For all cases, the PMI was calculated as the time elapsed between the reported time of death (documented by the police or judicial authorities) and the CT scan. The final study group consisted of 74 individuals (60 men, 14 women; age range 18–84 years; mean age, 41.8 ± 17.6 years) who underwent forensic autopsy. The CT images included in the study were selected to ensure artifact-free quality, a supine body position, preserved organ integrity, and appropriate postmortem preservation conditions (Figure 1).

PMCT images were independently evaluated by two radiologists for interobserver assessment.

Computed tomography

CT examinations were performed using a 64-detector array multislice CT scanner (LightSpeed VCT 64; GE Healthcare, Milwaukee, WI, USA). The imaging parameters for the brain and neck CT were as follows: tube voltage, 100 kV; tube current, 150–320 mAs; slice thickness, 2.5 mm; collimation, 64 × 0.625 mm; matrix, 512 × 512; rotation time, 0.5 seconds; and field of view (FOV), 250 mm. The imaging parameters for the thorax and abdomen CT were as follows: tube voltage, 140 kV; tube current, 150–320 mAs; slice thickness, 1.25 mm; collimation, 64 × 0.625 mm; matrix,

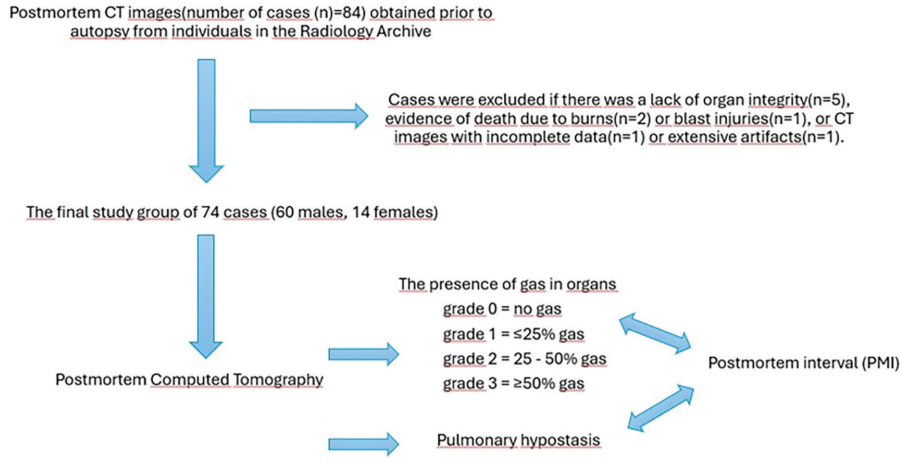


Figure 1. Flowchart of the relationship between hypostasis and gas detected in postmortem computed tomography and the postmortem interval. CT, computed tomography.

512 × 512; rotation time, 0.5 seconds; and FOV, 500 mm. All PMCT images were evaluated at the workstation in axial, sagittal, and coronal planes.

Image analysis

On postmortem brain CT, the presence of gas in intracranial vascular structures was assessed (Figure 2). On thoracic and abdominal PMCT, the presence of gas in the heart, liver, kidneys, and aorta was graded as follows: grade 0, no gas; grade 1, ≤ 25% gas; grade 2, > 25% but < 50% gas; and grade 3, ≥ 50% gas. These findings were compared with the PMI (Figures 3 and 4). On thoracic CT, the presence or absence of pulmonary hypostasis was assessed in the lung window. Density measurements were obtained using a region of interest of 500–600 mm^2 from lung parenchyma with and without hypostasis (Figure 5). In the mediastinal window, the presence of clotting in the pulmonary trunk or lobar pulmonary arteries was evaluated (Figure 6). The density of clots was also measured, and findings of hypostasis and clotting were compared with the PMI.

Statistical analysis

Data analysis was performed using SPSS software (version 27.0 for Windows; IBM Corp., Armonk, NY, USA). Descriptive statistics were presented as mean ± standard deviation for continuous variables and as frequencies and percentages for categorical variables. Chi-squared and Fisher's exact tests were used for categorical variables. Pearson correlation analyses were conducted to assess the relationships between hypostasis, clotting in the pulmonary arteries, and intravascular gas in organs. Independent samples t-tests were used to compare continuous variables. A P value <0.05 was considered statistically significant. An inter-observer reliability analysis with the Kappa statistic was performed to determine consistency among radiologists. Inter-observer agreement was categorized as follows: 0–0.20, slight; 0.21–0.40, moderate; 0.41–0.60, fair; 0.61–0.80, substantial; and 0.81–1.00, almost perfect.

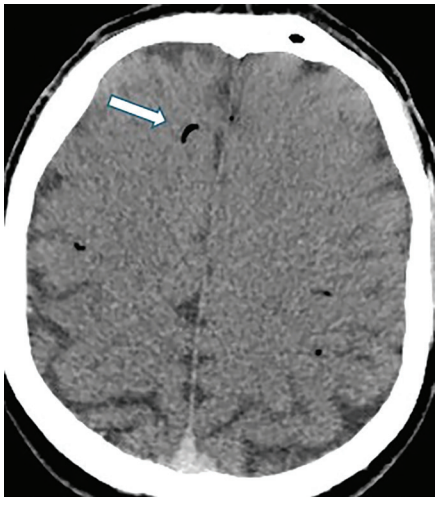


Figure 2. Intravascular gas (arrow) on non-contrast axial postmortem brain computed tomography.

Results

In the study group, 50 individuals (67.6%) died due to penetrating injuries caused by firearms or sharp objects, 14 (18.9%) due to blunt trauma or battery, 2 (2.7%) due to hanging or strangulation, and 8 (10.8%) from natural or medical causes. The PMIs of the cases in the study group were obtained through postmortem examination and autopsy findings, crime scene reports, and incident histories, and it was revealed that 35.1% died 0–7 hours prior to autopsy and 33.8% died 8–16 hours prior to autopsy.

Gas density was observed in the intracranial vascular structures in 66.2% of cases and in the cervical spinal canal in 44.6% of cases, with increasing frequency correlating with longer PMIs. Intravascular gas in the cardiac chambers was present in all cases except for seven individuals who died within 0–7 hours, and its frequency increased with time after death. The presence of clotting in the pulmonary arteries showed a statistically significant association with the PMI (P = 0.015). By contrast, there was no statistically significant relationship between the PMI and the presence of hypostasis in the lung parenchyma (P = 0.119) (Table 1).

A strong positive correlation (r: 0.720) was observed between intravascular gas in the liver and in the cardiac chambers. Furthermore, a moderate positive and statistically significant correlation was found between the PMI and the presence of intracranial intravascular gas, intravascular gas in the liver, gas in the cardiac chambers, and intravascular gas in the kidneys and aorta (Table 2).

Clots were identified in the pulmonary trunk and its branches in 35 cases. Clotting density ranged between 20 and 108 Hounsfield unit (HU). A statistically significant (P = 0.001) and strong positive correlation (r: 0.892) was found between pulmonary hypostasis and the presence of clots in the pulmonary arteries. The shared variance between these variables was calculated as 79.6%, indicating that approximately 79.6% of hypostasis could be explained by the presence of pulmonary arterial clotting (Table 3).

In density measurements, lung regions with hypostasis showed values ranging from -165 to -513 HU, whereas regions without hypostasis showed values ranging from -507 to -896 HU. A statistically significant and strong correlation was observed between pulmonary arterial clotting and the density differences between hypostatic and non-hypostatic lung parenchyma (r: 0.918) (Table 4). Interobserver reliability for detecting intraparenchymal and intravascular gas and pulmonary hypostasis on PMCT was found to be high (κ: 0.952–0.992).

Discussion

Determining the PMI is a critical component of criminal investigations.[7,8] In the present study, autopsy examinations together with law enforcement and judicial authority reports were used to establish the PMI. In our cohort, gas was observed in the heart in 73.1% and in the liver in 61.5% of corpses (n = 26) within 0–7 hours of death (r: 0.720). The amount of gas detected in the heart was greater than that in the liver. Previous studies have reported early intrahepatic and cardiac gas accumulation within the first postmortem hours;[9,10] our results support these findings, with higher levels of gas in the heart than in the liver. This might be explained by the greater elasticity of the right cardiac chambers than of the liver.

In this study, hepatic gas was detected in 81.1% of cases, except in those with very short PMIs. Jackowski et al.[11] reported hepatic gas in 59.5% of cases, whereas Takahashi et al.[12] reported a rate of 31.7%. Takahashi et al.[12] also found no correlation between intrahepatic gas and the PMI. By contrast, our results demonstrate a significant correlation between intravascular gas in the liver, heart, kidneys, and aorta with the PMI. Furthermore, cardiac gas was present in all corpses with a PMI of 0–7 hours, whereas hepatic and aortic gas were consistently detected in corpses with PMIs of 8–16 hours or longer. Ishida et al.[7] similarly reported that gas could be detected simultaneously in the liver, kidneys, spleen, and pancreas; in this study, gases in these organs also appeared approximately simultaneously.

Egger et al.[13] reported venous collapse in 61.9% and arterial collapse in 33.1% of the 118 PMCT images with PMIs of 3 hours to 12 days and also found a negative correlation between venous collapse and age. In this study, gas was absent in the aorta in 52.7% of cases; however, it was present in the aorta of all corpses with PMIs longer than 48 hours.

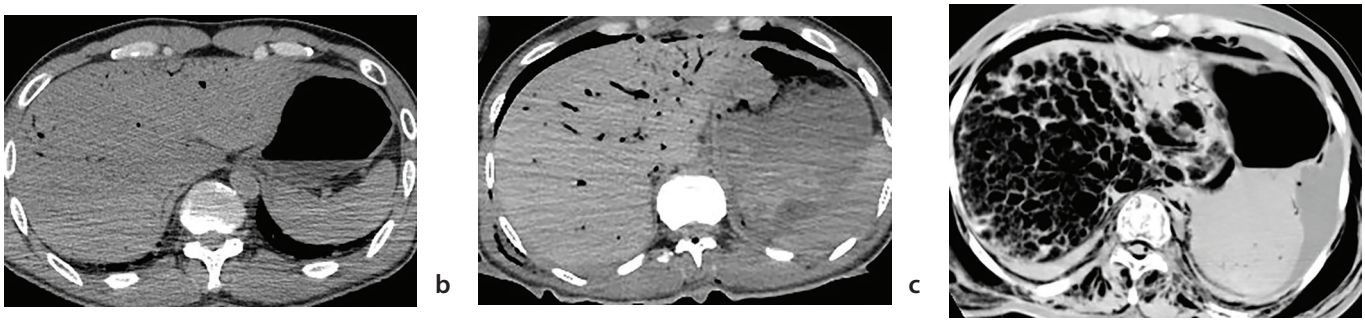


Figure 3. Intraparenchymal gas in the liver on non-contrast axial postmortem abdominal computed tomography, shown as **(a)** grade 1, **(b)** grade 2, and **(c)** grade 3.

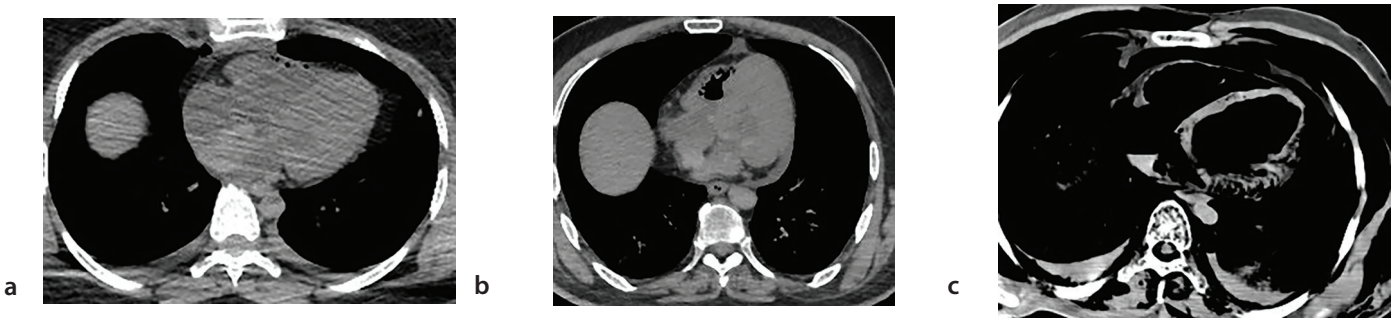


Figure 4. Gas in the cardiac chambers on non-contrast axial postmortem thoracic computed tomography, shown as **(a)** grade 1, **(b)** grade 2, and **(c)** grade 3.

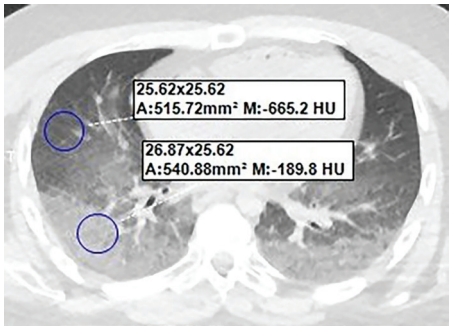


Figure 5. Increased attenutation in the dependent portions of both lungs on non-contrast axial postmortem thoracic computed tomography, consistent with hypostasis. Density measurements were obtained using a region of interest of 500–600 mm^2 from lung parenchyma with and without hypostasis. HU, Hounsfield unit.

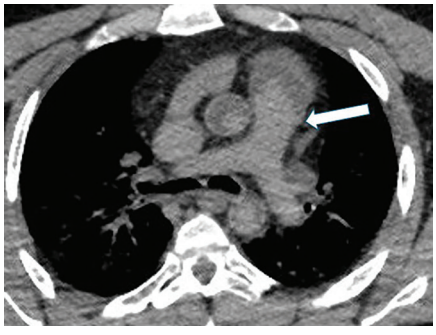


Figure 6. Hyperdense clotting in the pulmonary trunk and lobar pulmonary arteries on non-contrast axial postmortem thoracic computed tomography (arrow).

Cartocci et al.[14] evaluated 41 corpses with PMIs ranging from 4 to 930 days, correlating external decomposition with the radiological alteration index (RAI) on PMCT. They found that gas above grade 2 in the heart, liver, and major vessels was associated with an RAI score > 61, which corresponded to moderate-to-severe putrefaction. Additionally, 54% of cases demonstrated more than 50% intracranial gas.[14] In another study of 159 PMCTs, intracranial gas was identified in 62 corpses, and 40.2% of these cases were reported as having intravascular gas.[15] In this study, we did not grade the extent of intracranial intravascular gas. However, we observed gas in intracranial vessels in 34.6% of corpses with a PMI of 0–7 hours and in all corpses with PMIs greater than 48 hours.

The most common pulmonary finding on PMCT is hypostasis, which develops as a result of the loss of tone in the respiratory muscles and diaphragm after death. The expiratory position of the diaphragm in the postmortem period further contributes to attenuation differences in the basal lung regions.[16] In this study, we evaluated the relationship between hypostasis detected on PMCT and the PMI. Hypostasis was observed in 47.3% of our study group but was absent in corpses with a PMI exceeding 72 hours.

Jackowski et al.[11] reported hypostasis in 79.5% of cases on PMCT and magnetic resonance imaging (MRI). In a study by Tumanova et al.,[4] MRI examinations of 62 newborns and infants with PMIs of 0–72 hours were assessed. The PMIs were stratified, and hypostasis was compared with the PMI according to MR signal gradient differences. Hypostasis-related MR signal changes were detected in 57.1% of cases at 0–6 hours and 33% at 6–12 hours, with the strongest signal gradient consistent with hypostasis detected in 75% of cases at 18–24 hours.[4] Similarly, Kinoshita et al.[5] evaluated four pigs at hourly intervals for 24 hours postmortem. Based on density measurements from the dorsal and ventral lung regions, attenuation differences began to appear in the dorsal regions at hour 8 and continued to increase until 24 hours. Although significant differences were noted between baseline and later measurements, no significant changes were observed between 8 and 24 hours.[5] In this study, hypostasis was observed with increasing frequency up to 48 hours and in corpses with a PMI of 48–72 hours.

Matsuyama et al.[17] evaluated antemortem and postmortem lung CT images in nine rats scanned in the prone position. They reported a transient decrease in lung volume with a temporary increase in tracheal and bronchial volumes. Pulmonary congestion and consolidations were identified at 48 hours postmortem, although interstitial parenchymal

Table 1. Relationship between the postmortem interval and gas detected in organs, lung hypostasis, and pulmonary artery clotting on postmortem computed tomography

Postmortem computed tomography		Postmortem interval							
		0–7 hours	8–16 hours	17–48 hours	48–72 hours	73–120 hours	> 120 hours		*P*
Intravascular gas in the cranium	Negative	17 (23%)	5 (6.8%)	3 (4.1%)	0	0	0	25 (33.8%)	0.002
	Positive	9 (12.2%)	20 (27%)	12 (16.2%)	4 (5.4%)	1 (1.4%)	3 (4.1%)	49 (66.2%)	
Intracardiac gas	Absent	7 (9.5%)	0	0	0	0	0	7 (9.5%)	0.000
	Grade 1	13 (17.6%)	5 (6.8%)	3 (4.1%)	0 (0%)	0 (0%)	0	21 (28.4%)	
	Grade 2	6 (8.1%)	13 (17.6%)	6 (8.1%)	0	0	0	25 (33.8%)	
	Grade 3	0	7 (9.5%)	6 (8.1%)	4 (5.4%)	1 (1.4%)	3 (4.1%)	21 (28.4%)	
Intravascular gas in the liver	Absent	10 (13.5%)	4 (5.4%)	0	0	0	0	14 (18.9%)	0.000
	Grade 1	10 (13.5%)	5 (6.8%)	3 (4.1%)	0	0	0	18 (24.3%)	
	Grade 2	5 (6.8%)	15 (20.3%)	11 (14.9%)	1 (1.4%)	0	0	32 (43.2%)	
	Grade 3	1 (1.4%)	1 (1.4%)	1 (1.4%)	3 (4.1%)	1 (1.4%)	3 (4.1%)	10 (13.5%)	
Intravascular gas in the aorta	Absent	21 (28.4%)	12 (16.2%)	6 (8.1%)	0	0	0	39 (52.7%)	0.000
	Grade 1	4 (5.4%)	4 (5.4%)	4 (5.4%)	0	0	0	12 (16.2%)	
	Grade 2	0	3 (4.1%)	1 (1.4%)	0	0	0	4 (5.4%)	
	Grade 3	1 (1.4%)	6 (8.1%)	4 (5.4%)	4 (5.4%)	1 (1.4%)	3 (4.1%)	19 (25.7%)	
Intravascular gas in the kidney	Absent	24 (32.4%)	18 (24.3%)	8 (10.8%)	2 (2.7%)	0	0	52 (70.3%)	0.000
	Grade 1	1 (1.4%)	5 (6.8%)	4 (5.4%)	0	0	0	10 (13.5%)	
	Grade 2	1 (1.4%)	2 (2.7%)	2 (2.7%)	0	0	0	5 (6.8%)	
	Grade 3	0	0	1 (1.4%)	2 (2.7%)	1 (1.4%)	3 (4.1%)	7 (9.5%)	
Clotting in the pulmonary artery	Negative	8 (10.8%)	18 (24.3%)	6 (8.1%)	3 (4.1%)	1 (1.4%)	3 (4.1%)	39 (52.7%)	0.015
	Positive	18 (24.3%)	7 (9.5%)	9 (12.2%)	1 (1.4%)	0	0	35 (47.3%)	
Hypostasis	Negative	10 (13.5%)	16 (21.6%)	6 (8.1%)	3 (4.1%)	1 (1.4%)	3 (4.1%)	39 (52.7%)	0.119
	Positive	16 (21.6%)	9 (12.2%)	9 (12.2%)	1 (1.4%)	0	0	35 (47.3%)	
Total		26 (35.1%)	25 (33.8%)	15 (20.3%)	4 (5.4%)	1 (1.4%)	3 (4.1%)	74 (100%)	

Table 2. Correlation analysis between gas detected in organs and the postmortem interval on postmortem computed tomography

		Postmortem interval	Intravascular gas in the cranium	Intravascular gas in the liver	Intravascular gas in the kidney	Intracardiac gas	Intravascular gas in the aorta
Postmortem interval	Pearson r	1	0.419	0.624	0.658	0.636	0.585
	P		0.000	0.000	0.000	0.000	0.000
Intravascular gas in the cranium	Pearson r		1	0.477	0.318	0.607	0.429
	P			0.000	0.006	0.000	0.000
Intravascular gas in the liver	Pearson r			1	0.599	0.720	0.568
	P				0.000	0.000	0.000
Intravascular gas in the kidney	Pearson r				1	0.505	0.638
	P					0.000	0.000
Intracardiac gas	Pearson r					1	0.621
	P						0.000

Table 3. Relationship between the presence of pulmonary arterial clotting and lung hypostasis on postmortem computed tomography

		Clotting in the pulmonary artery	
		Positive	Negative
Hypostasis	Positive	37 (50%)	2 (2.7%)
	Negative	2 (2.7%)	33 (44.6%)
Total		39 (52.7%)	35 (47.3%)
P		*P* = 0.001	
			Hypostasis
Clotting in the pulmonary artery		Pearson r	0.892
		P	0.001
		n	74

Table 4. Correlation analysis between pulmonary hypostasis and pulmonary arterial clotting on postmortem computed tomography

		Density of hypostatic parenchyma	Density of non-hypostatic parenchyma	Pulmonary artery clotting	Pulmonary artery clotting density
Density of hypostatic parenchyma	Pearson r	1	0.918	0.831	0.697
	P		0.000	0.000	0.000
Density of non-hypostatic parenchyma	Pearson r		1	0.889	0.748
	P			0.000	0.000
Pulmonary artery clotting	Pearson r			1	0.880
	P				0.000

changes could not be assessed due to the small lung volume.[17] Although we did not assess the trachea and bronchi morphologically in this study, we observed that hypostasis increased particularly in corpses with PMIs of 0–72 hours.

Pulmonary clotting is seen on CT as hyperdense intraluminal clots without fluid–fluid levels.[18,19] In our cohort, clots were detected in 35 cases within the pulmonary trunk or its branches. A statistically significant ($P = 0.001$) and strong positive correlation (r: 0.892) was found between hypostasis and the presence of pulmonary arterial clotting. No signs of hypostasis were observed in corpses with collapsed pulmonary arteries or intravascular gas in the pulmonary arteries. Accordingly, we suggest that pulmonary hypostasis may develop as a consequence of clotting or sedimentation within the pulmonary arteries.

This study has several limitations. First, the number of cases included was relatively small. Accordingly, no significant relationship was found between hypostasis and the PMI in this study. We believe that a larger sample size might reveal a statistically significant difference regarding hypostasis. Second, the PMI was estimated based on autopsy findings and law enforcement reports, which may introduce bias. Third, external factors such as environmental conditions (e.g., hot and humid weather during summer) and the time taken for corpses to be transported from the field to CT and autopsy may have affected the PMI. High ambient temperatures during the summer accelerate the decomposition process, and in this study, the PMI values of bodies found in this period were relatively short. The forensic cause of death and positional changes occurring during the postmortem period may also influence the development of hypostasis. Therefore, in this study, particular attention was paid to ensuring complete body integrity and that all bodies were found in the supine position. Finally, information regarding chronic diseases, sepsis, or infections in the study group was unavailable.

In conclusion, on PMCT, decomposition-related gas can be detected in solid organs, particularly in the liver and heart, as early as within 48 hours postmortem. A moderate correlation exists between gas detected on PMCT and the PMI. Additionally, a strong correlation was observed between clotting or sedimentation in the pulmonary arteries and pulmonary hypostasis on PMCT.

Footnotes

Conflict of interest disclosure

The authors declared no conflicts of interest.

References

1. Decker SJ, Braileanu M, Dey C, et al. Forensic radiology: a primer. *Acad Radiol*. 2019;26(6):820-830. [Crossref]
2. Klein WM, Bosboom DG, Koopmanschap DH, Nievelstein RA, Nikkels PG, van Rijn RR. Normal pediatric postmortem CT appearances. *Pediatr Radiol*. 2015;45(4):517-526. [Crossref]
3. Del Fante Z, De Matteis A, Fazio V, et al. The importance of post mortem computed tomography (PMCT) in the reconstruction of the bullet trajectory. *Clin Ter*. 2019;170(2):129-133. [Crossref]
4. Tumanova UN, Bychenko VG, Serova NS, Shchegolev AI. Postmortem MRI characterization of cadaveric hypostases in deceased newborns. *Bull Exp Biol Med*. 2021;170(3):371-377. [Crossref]
5. Kinoshita K, Sakai T, Inai K, et al. Postmortem temporal chest CT and its pathological correlation in piglets. *J Med Invest*. 2024;71(3-4):232-236. [Crossref]
6. Shenton A, Kralt P, Suvarna SK. Death, post mortem changes and decomposition on post mortem computed tomography. In: Shenton A, Kralt P, Suvarna SK, eds. Post mortem CT for non-suspicious adult death. Cham: Springer; 2021:50-56. [Crossref]
7. Ishida M, Gonoi W, Hagiwara K, et al. Intravascular gas distribution in the upper abdomen of non-traumatic in-hospital death cases on postmortem computed tomography. *Leg Med (Tokyo)*. 2011;13(4):174-179. [Crossref]
8. Romanelli MC, Marrone M, Veneziani A, et al. Hypostasis and time since death: state of the art in Italy and a novel approach for an operative instrumental protocol. *Am J Forensic Med Pathol*. 2015;36(2):99-103. [Crossref]
9. Fischer F, Grimm J, Kirchhoff C, Reiser MF, Graw M, Kirchhoff S. Postmortem 24-h interval computed tomography findings on intrahepatic gas development and changes of liver parenchyma radiopacity. *Forensic Sci Int*. 2012;214(1-3):118-123. [Crossref]
10. Egger C, Bize P, Vaucher P, et al. Distribution of artifactual gas on post-mortem multidetector computed tomography (MDCT). *Int J Legal Med*. 2012;126(1):3-12. [Crossref]
11. Jackowski C, Sonnenschein M, Thali MJ, et al. Intrahepatic gas at postmortem computed tomography: forensic experience as a potential guide for in vivo trauma imaging. *J Trauma*. 2007;62(4):979-988. [Crossref]
12. Takahashi N, Higuchi T, Shiotani M, Maeda H, Hirose Y. Intrahepatic gas at postmortem multislice computed tomography in cases of nontraumatic death. *Jpn J Radiol*. 2009;27(7):264-268. [Crossref]
13. Egger C, Wiskott K, Vaucher P, et al. Postmortem changes of the vascular system: a thanatological study using multidetector computed tomography. *Int J Legal Med*. 2023;137(4):1109-1115. [Crossref]
14. Cartocci G, Santurro A, Neri M, et al. Postmortem computed tomography (PMCT) radiological findings and assessment in advanced decomposed bodies. *Radiol Med*. 2019;124(11):1018-1027. [Crossref]
15. Borowska-Solonynko A, Koczyk K, Blacha K, Prokopowicz V. Significance of intracranial gas on post-mortem computed tomography in traumatic cases in the context of medico-legal opinions. *Forensic Sci Med Pathol*. 2020;16(1):3-11. [Crossref]
16. Filograna L, Thali MJ. Post-mortem CT imaging of the lungs: pathological versus

non-pathological findings. *Radiol Med*. 2017;122(12):902-908. [Crossref]

17. Matsuyama T, Ota S, Inui Y, et al. Examination of postmortem changes in the lungs, trachea, and bronchi in a rat model imaged with small-animal computed tomography. *Fujita Med J*. 2023;9(2):101-104. [Crossref]
18. Ishida M, Gonoi W, Okuma H, et al. Common Postmortem computed tomography findings following atraumatic death: differentiation between normal postmortem changes and pathologic lesions. *Korean J Radiol*. 2015;16(4):798-809. [Crossref]
19. Offiah CE, Dean J. Post-mortem CT and MRI: appropriate post-mortem imaging appearances and changes related to cardiopulmonary resuscitation. *Br J Radiol*. 2016;89(1058):2015085. [Crossref]